Digital Discovery

ROYAL SOCIETY OF CHEMISTRY

PAPER

Cite this: DOI: 10.1039/d6dd00136j

Evaluating global optimization and generative methods for low-energy and diverse crystal structure prediction *via* two case studies

Sunggi An,†[a] Sungwon Kim,†[b] Jinyoung Ko,[c] Juhwan Noh,[d] Zahed Allahyari,[e] Artem R. Oganov,*[f] Alán Aspuru-Guzik,*[ghi] Chris J. Pickard*[jk] and Yousung Jung*[cl]

Accurate crystal structure prediction (CSP) is essential for discovering novel materials. Although various CSP methods have been developed, systematic benchmarks and quantitative comparisons remain limited. In this study, we evaluate eight CSP approaches: the evolutionary algorithm USPEX, three versions of *ab initio* random sampling with symmetry constraints (USPEX, AIRSS, and PyXtal codes), generative machine learning models (generative adversarial neural network, GAN, and variational autoencoder, VAE), and two very different template-based structure generators (random topological structure generator of USPEX and CSPML). These tests are done through a case study on vanadium oxide systems V_5O_8 and V_3O_4. Our results show that most of the compared methods are capable of identifying low-energy and metastable structures when sufficient sampling is performed. However, each method exhibits distinct strengths and trade-offs in terms of accuracy, efficiency, structural diversity, and symmetry character. Notably, more established traditional methods, such as USPEX and AIRSS, offer robust performance across system sizes, while ML-based approaches demonstrate rapid structure generation with minimal sampling, albeit with a greater reliance on the quality of the training data and post-processing approaches. Interestingly, different versions of random sampling show very different performances. This study underscores the complementary nature of traditional and ML-based CSP strategies and provides practical guidance for selecting appropriate methods based on the complexity of the system, the computational resources available, and the specific discovery objectives.

Received 24th March 2026
Accepted 27th June 2026

DOI: 10.1039/d6dd00136j

rsc.li/digitaldiscovery

1. Introduction

Crystal structure prediction (CSP) is essential for understanding and designing materials, as the properties of a given ordered material are closely tied to its crystal structure. CSP remains challenging due to complex energy landscapes and large search spaces. Soon after crystal structure determinations became possible, simple heuristic rules were formulated, capable of discriminating between realistic and unlikely crystal structures.[1] Modern CSP methods[2] incorporate advanced global optimization algorithms, such as basin hopping,[3] simulated annealing,[4,5] and evolutionary algorithms,[6–9] combined with first-principles calculations, particularly density functional theory (DFT). These techniques aim to identify the global energy minimum structure and metastable polymorphs with potentially useful properties.

Among the various CSP techniques, two major CSP approaches, Evolutionary Algorithms (EAs) and *Ab Initio* Random Structure Search (AIRSS), have shown strong performance in predicting complex structures, including those of super-hard materials[10] and superconductors.[11,12] In contrast, and more recently, machine learning (ML)-based methods[13]

[a]*Department of Chemical and Biomolecular Engineering, Korea Advanced Institute of Science and Technology (KAIST), Daejeon, Republic of Korea*
[b]*Samsung Advanced Institute of Technology, Suwon 16678, South Korea*
[c]*Department of Chemical and Biological Engineering, Institute of Chemical Processes, Seoul National University, Seoul 08826, South Korea. E-mail: yousung.jung@snu.ac.kr*
[d]*Korea Research Institute of Chemical Technology (KRICT), Daejeon, 34114, Republic of Korea*
[e]*VASP Software GmbH, Berggasse 21/14, A-1090 Vienna, Austria*
[f]*Skolkovo Institute of Science and Technology, 30 Bldg. 1 Bolshoy Blvd., 121205 Moscow, Russia. E-mail: A.Oganov@skoltech.ru*
[g]*Department of Computer Science, University of Toronto, 40 St George St., Toronto, ON M5S 2E4, Canada. E-mail: aspuru@utoronto.ca*
[h]*Department of Chemistry, University of Toronto, 80 St. George St., Toronto, ON M5S 3H6, Canada*
[i]*Vector Institute for Artificial Intelligence, W1140-108 College St., Schwartz Reisman Innovation Campus, Toronto, ON M5G 0C6, Canada*
[j]*Department of Materials Science and Metallurgy, University of Cambridge, 27 Charles Babbage Road, Cambridge CB30FS, UK. E-mail: cjp20@cam.ac.uk*
[k]*Advanced Institute for Materials Research, Tohoku University, Sendai, 980-8577, Japan*
[l]*Institute of Engineering Research, Seoul National University, Seoul 08826, South Korea*
† These authors contributed equally to this work.

leveraging large crystal structure databases,[14–20] have emerged to enhance energy evaluations and accelerate structure generation. These approaches often utilize machine learning potentials and deep generative models.[13,17,18,21]

Despite the growing number of CSP methodologies, including data-driven ML models,[22] a comprehensive benchmarking and systematic comparison of their performance remains underexplored. This study aims to fill the gap by conducting a detailed case study comparing several CSP methods in predicting the stability and structural diversity of vanadium-oxide polymorphs, V_5O_8 and V_3O_4. We evaluate eight representative methods: evolutionary algorithm USPEX (Universal Structure Predictor: Evolutionary Xtallography),[8] random symmetric structure generator of USPEX (USPEX-randSymm),[23] random topological structure generator of USPEX (USPEX-randTop),[24] *Ab initio* Random Structure Searching (AIRSS),[25,26] iMatGen,[18] composition-conditioned crystal GAN,[17] PyXftal,[19] and CSPML.[20] By analyzing their predictive accuracy and ability to generate diverse structures, this study aims to clarify the strengths and limitations of each approach and provide guidance for future CSP research and applications.

However, CSP benchmarking should not be interpreted as a direct measure of materials-discovery success. While finding low-energy and diverse metastable structures is important, experimental realization also depends on synthetic accessibility, kinetic pathways, processing conditions, and target properties. Therefore, we evaluate CSP performance mainly in terms of thermodynamic search efficiency, metastable-structure sampling, and structural-diversity coverage.

This view motivates evaluation beyond recovering a single ground-state structure. In addition to global-minimum discovery, we analyze distributional features of the generated structures, including metastable-structure fractions, energy distributions, chemical-space coverage, and space-group diversity. These descriptors clarify the sampling behavior of each method and are useful when multiple plausible polymorphs are of interest.

2. Methods

We chose the V–O system for comparing CSP methods due to vanadium's wide range of oxidation states (+2 to +5) and its rich structural diversity, featuring varying oxygen coordination environments. This rich chemistry makes vanadium oxides ideal candidates for generating multiple polymorphs and metastable structures.[18] Moreover, vanadium oxides are used as catalysts and are promising for applications in ion batteries, water splitting, smart windows, supercapacitors, memristors, and sensors.[39] Previous studies using data-driven CSP methods have successfully identified several new vanadium oxide polymorphs with low energies close to the convex hull, indicating their near-stable or metastable nature.[18] Building on this, the present study compares those previously reported structures with the polymorphs produced by various other CSP methodologies, aiming to analyze the performance and characteristics of each method in exploring the structural landscape of vanadium oxides.

We relaxed the structures using a consistent DFT method and conditions to ensure a standardized comparison (Table S1). To compare structural similarity and identify space groups, we used the StructureMatcher and SpacegroupAnalyzer functions in the Pymatgen Python package, applying default parameter settings.[27] The full details of standardized DFT calculation settings are summarized in the SI.

2.1 CSP methodologies compared in this work

In this study, we employed eight CSP methodologies (USPEX-EA, USPEX-randSym, USPEX-randTop, AIRSS, crystal GAN, iMatGen, PyXtal, and CSPML) to generate the crystal structures of V_5O_8 and V_3O_4 (Table 1). USPEX-EA, stands for a full evolutionary calculation using USPEX, a widely used *ab initio* evolutionary algorithm package for CSP, in its standard mode. USPEX searches for the global energy minimum, en route sampling a number of low-energy structures.

AIRSS (denoted here as RSS) is an *ab initio* random structure search method that generates chemically sensible random structures under given chemical compositions and a set of constraints. These structures are then optimized using DFT to identify low-energy configurations, including the global minimum. AIRSS is known for its simplicity, efficiency, and ability to generate quasi-random structures with specific rules (*e.g.*, symmetry, volume, coordination, structural units, and chemically sensitive minimum distances). Due to its randomness and broad sampling capability, AIRSS is commonly used in recent studies to generate diverse initial structures in a high-throughput manner.[28] Parallel implementation of USPEX and AIRSS further enhances their practicality for large-scale searches. We have included two other versions of random sampling: USPEX-randSym (randSym) and PyXtal. The former is usually used as part of evolutionary searches in USPEX, but was also tested separately here. PyXtal is another implementation of the same idea. It generates random crystal structures *ab initio* by starting from a given chemical composition, symmetry, and stoichiometry. The process uses special Wyckoff positions to generate 3D crystal structures. The unit cells are derived from Bravais lattices, with additional constraints applied to allow for possible extra lattice positions. Further DFT geometry optimization is required for relaxed crystal geometries. In this study, within PyXtal, we generated 8 random structures for each possible space group of a given composition.

The composition-conditioned crystal GAN (GAN) approach employs a Wasserstein GAN with gradient penalty (WGAN-GP),[29] conditioned on chemical composition, to generate novel crystal structures. This data-driven approach is trained on a virtual V_xO_y crystal structure database from the Materials Project. The model comprises a generator, discriminator, and classifier network. Structures are represented using rescaled-fractional coordinates as input features. To improve the model's robustness and representation invariance, data augmentation through supercell, translation, and rotation operations is applied during training. The generated structures are subsequently relaxed by DFT structural optimization, following the procedures outlined in the original study.

iMatGen (denoted as VAE) is based on a Variational Auto-Encoder (VAE).[30] In this approach, crystal structures are represented as 3D atomic density images, which are compressed into a 1D vector through an auto-encoder. The VAE is trained on these latent representations, effectively compressing the structural information into a lower-dimensional space. During this training process, stable and unstable regions are divided in the latent space, and the crystal structures to be generated are sampled from these stable regions.

CSPML is a substitution-based crystal structure generation method that uses a binary classification neural network to predict structural compatibility. For a given query composition, CSPML selects suitable template structures and performs atomic substitutions using compositionally and structurally similar candidates. The model is trained on 33 153 stable compounds from the Materials Project database, and learns to predict whether two compositions are likely to adopt similar crystal structures. This enables efficient generation of plausible structures based on known templates. A very different template crystal structure prediction method is the random topological crystal structure generator of USPEX (USPEX-randTop or, simply, randTop). Again, this is usually used as part of evolutionary USPEX searches, but here it was also tested as a separate method. Starting from a set of ideal nets, this generator corrects stoichiometry by symmetric substitution and addition of low-coordination atoms – this way, one can derive an infinite number of structures from each ideal net, and these structures very often possess low energy.[38]

3. Results

3.1 Discoverability of the ground state structure (finding the global minimum)

The primary goal of CSP is to identify the global minimum structure, representing the most thermodynamically stable configuration for a given chemical composition. To evaluate this capability, we compared the lowest energy structures identified by eight different CSP methodologies for V–O systems.

As shown in Table 2, six out of eight methods successfully identified the same global minimum structure for V_5O_8, and five out of eight did so for V_3O_4. Although PyXtal did not recover the ground state structure, its generative nature has the potential to find it through additional sampling. The CSPML model also failed to find the lowest energy structure for V_3O_4, but did identify a structure with a comparable energy. Its performance for V_5O_8 was more limited, likely due to the small number of template structures available for substitution (20 for V_3O_4 *vs.* 4 for V_5O_8). Overall, the remaining models demonstrated strong performance in locating low-energy structures across both compositions.

Table 2 A table showing whether CSP methodologies have discovered the global minimum structure in V_5O_8 and V_3O_4 respectively. For V_5O_8, six methodologies could discover the global minimum, and for V_3O_4, only five methodologies could discover the global minimum

Method	EA	randSym	randTop	RSS	GAN	VAE	PyXtal	CSPML
V_5O_8	+	+	+	+	+	+	–	–
V_3O_4	+	+	–	+	+	+	–	–

In the present setting, PyXtal's failure to recover the stable structure likely reflects its random symmetry- and Wyckoff-position-based sampling under a finite sampling budget, rather than an intrinsic limitation of the PyXtal framework. Low-energy vanadium oxides may require specific local V–O coordination motifs, oxidation-state preferences, or distorted polyhedral environments, which are not explicitly imposed during the initial PyXtal generation step.

The XRD patterns of the lowest energy structures for V_5O_8 and V_3O_4 are shown in Fig. S1 and S2, respectively. Notably, different methodologies identified the same ground-state structures, demonstrating both the consistency and reliability of these approaches. Interestingly, the VAE-based method (iMatGen) successfully discovered the ground state structure for both compositions, despite sampling a limited number of structures. This result highlights the efficiency of sampling within the stable region of the latent space, as commonly employed by many VAE-based crystal structure generative models.[31,32]

3.2 Discoverability of unique metastable polymorphs

Metastable structures, which are kinetically trapped phases with a higher free energy than the global ground state, are

Table 1 List of crystal structure prediction methodologies benchmarked in this work

Name	Initial guess structure/data sampling	Method of CSP	Reference
EA	Fully random structure generator	Evolutionary algorithm (USPEX)	Oganov & Glass[8]
randSym	Symmetry based random structure generator	Evolutionary algorithm (USPEX)	Lyakhov *et al.*[23]
randTop	Topology based random structure generator	Evolutionary algorithm (USPEX)	Bushlanov *et al.*[24]
RSS	Constrained random structures	*Ab initio* random structure search	Pickard *et al.*[26]
GAN	Composition-conditioned sampling from latent space	Deep generative model (composition-conditioned crystal GAN)	Kim *et al.*[17]
VAE	Random sampling from a stable region of stability-learned latent space	Deep generative model (iMatGen)	Noh *et al.*[18]
PyXtal	Random structures in a Bravais lattice & random Wyckoff position sampling	Python library for crystal structure generation and symmetry analysis (PyXtal)	Fredericks *et al.*[19]
CSPML	Substitution using structurally similar materials as a template	Crystal structure prediction with machine learning-based element substitution (CSPML)	Kusaba *et al.*[20]

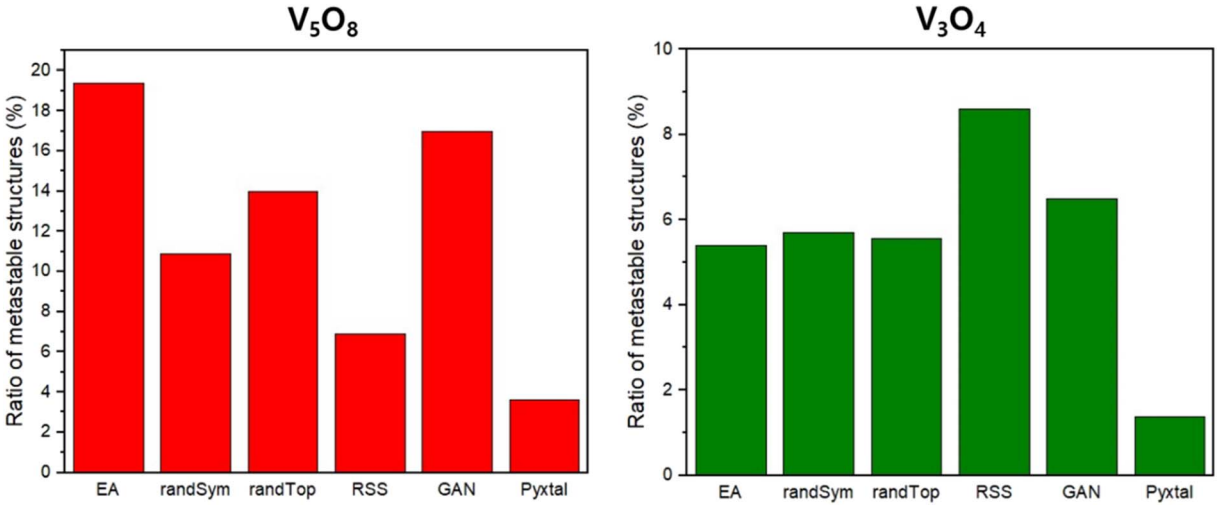

Fig. 1 The ratio of metastable polymorphs discovered by CSP methodologies. Metastable polymorphs were defined as structurally unique DFT-relaxed structures with an energy above the convex hull (E_{hull}) of less than 200 meV per atom. The ratio was calculated using the number of such metastable structures generated by each method as the numerator and the total number of DFT-relaxed valid structures generated by the same method as the denominator.

frequently observed in nature. Many technologically interesting materials are metastable,[33] hence the importance of having algorithms capable of predicting metastable states. To assess each CSP model's ability to discover such structures, we analyzed both the discoverability ratio and the energy distributions of metastable structures. In this study, metastable structures are defined as those with moderately low formation energies, specifically with energy above the convex hull (E_{hull}) less than 200 meV per atom.[33]

The results are shown in Fig. 1, with the VAE and CSPML methods excluded from the analysis due to their different sampling methods and limited structure generation. Among the remaining methods, EA and RSS showed the highest ratios of metastable structures in V_5O_8 and V_3O_4. As shown in Fig. 2, we plotted the energies above the convex hull, where lower values indicate greater thermodynamic stability. Metastable structures appear above the ground state but within the defined threshold of 200 meV per atom. Except for VAE, PyXtal, and CSPML, all other methods generated a wide distribution of polymorphs within this metastable range. This suggests that the five CSP methods (EA, randSym, randTop, RSS, GAN, and VAE) generally possess a strong capability for generating a diverse set of metastable polymorphs. This suggests that, under the present sampling budget, PyXtal did not frequently generate initial structures close enough to the distorted V–O motifs needed for low-energy basins.

The VAE method generates structures by random sampling within the stable regions of the latent space, resulting in a relatively small number of polymorphs for V_5O_8 and V_3O_4. However, the energy distribution of these structures was more thermodynamically stable compared to those from other methods, consistent with the success of VAE in identifying the global minimum structures. On the other hand, PyXtal produced a variety of high-energy structures that were too diverse to yield metastable structures effectively (Fig. S3). The GAN model showed the second-best performance overall, indicating that deep generative models can perform comparably to traditional CSP methods in discovering low-energy and metastable structures.

3.3 Coverage on V_xO_y chemical space

Structural diversity is a key aspect of CSP methods, particularly in population-based approaches like genetic algorithms, which explicitly promote diversity to prevent premature convergence. Thus, quantitatively comparing structural diversity across data-driven models, random structure search methods, and other approaches is highly valuable. To assess and compare this diversity, we evaluated the structural space coverage of each method, following the approach proposed by Reinhardt *et al.*[34] with the goal of maximizing diversity and minimizing redundancy in the generated structures.

First, we represented the metastable structures using the Smooth Overlap of Atomic Positions (SOAP),[35] and projected these high-dimensional vectors into a two-dimensional space using t-Stochastic Neighbor Embedding (t-SNE).[36] Next, we applied Density-Based Spatial Clustering of Applications with Noise (DBSCAN)[37] to identify clusters in the projected spaces.[34] This overall process of mapping and clustering is illustrated in Fig. 3.

To evaluate chemical space coverage, we measured how many DBSCAN clusters included at least one polymorph generated by each method. The number of clusters covered served as a metric for the extent of chemical space exploration. To ensure robustness, we repeated the analysis using three different DBSCAN parameter sets for each composition.

The results, summarized in Tables 3 and 4, indicate that for V_5O_8, the EA method consistently achieved the highest chemical space coverage across all parameter sets (Fig. S8–S13). For V_3O_4,

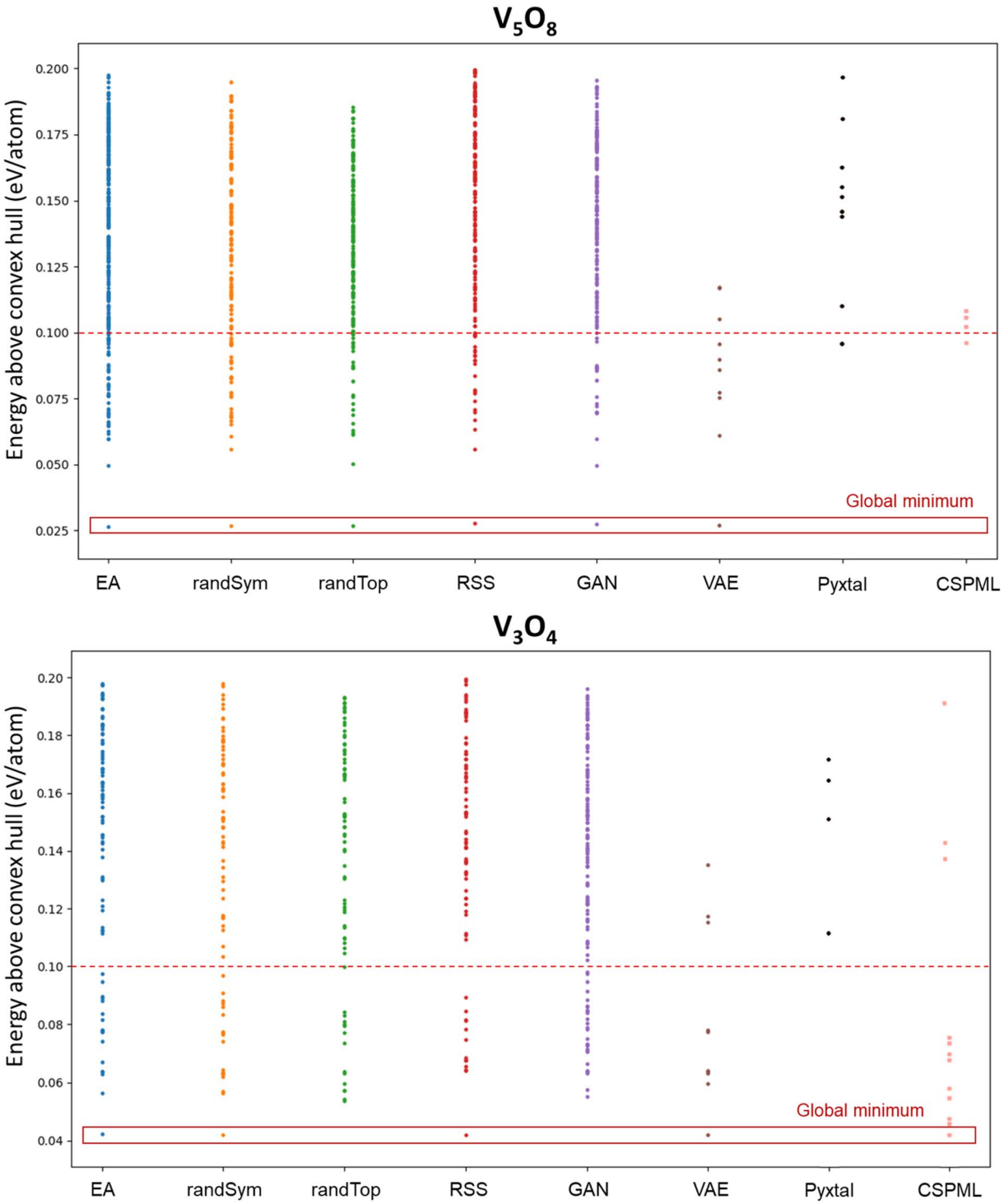

Fig. 2 The energy distribution of metastable polymorphs discovered by CSP methodologies. Each data point corresponds to a DFT-relaxed structure generated for the V_5O_8 or V_3O_4 composition after duplicate structures were removed by structural matching. The *y*-axis reports the energy above the convex hull (E_{hull}), and structures with E_{hull} < 200 meV per atom were considered metastable in this analysis. The red dotted line denotes the stricter 100 meV per atom threshold.

both EA and GAN-based methods showed similar high coverage. The VAE, PyXtal, and CSPML results were excluded from the analysis due to the insufficient number of metastable structures generated.

These findings suggest that structure generation methods with fewer initial constraints, such as EA and GAN, tend to promote greater structural diversity. However, it is important to note that these conclusions are based on relatively small systems, and in larger systems, the influence of initial

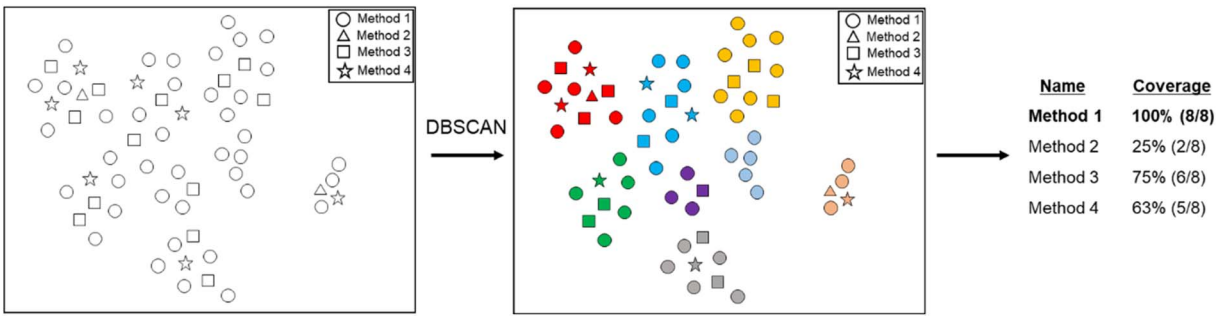

Fig. 3 Schematic example of measuring the coverage of each method by clustering the data points on the chemical space. Structurally unique metastable polymorphs were represented by SOAP descriptors, projected into two dimensions using t-SNE, and clustered using DBSCAN. A method was considered to occupy a cluster if at least one metastable structure generated by that method belonged to the cluster.

Table 3 The number of DBSCAN clusters occupied by V_5O_8 structures of each CSP method. "Parameters" is the parameters of DBSCAN. "# of total clusters" means the total number of clusters formed with certain "Parameters". The number of clusters according to DBSCAN, in parentheses, is the ratio of occupied clusters

Parameters (ε, $\min_{points}$)	# of total clusters	EA	randSym	randTop	RSS	GAN
$\varepsilon = 4$, $\min_{points} = 5$	30	**30 (100.0%)**	23 (76.7%)	26 (86.7%)	23 (76.7%)	24 (80.0%)
$\varepsilon = 3$, $\min_{points} = 5$	58	**58 (100.0%)**	42 (72.4%)	50 (86.2%)	36 (62.1%)	44 (75.9%)
$\varepsilon = 3$, $\min_{points} = 4$	69	**67 (97.1%)**	48 (69.6%)	61 (88.4%)	43 (62.3%)	50 (72.5%)

Table 4 The number of DBSCAN clusters occupied by V_3O_4 structures of each CSP method. "Parameters" is the parameters of DBSCAN. "# of total clusters" means the total number of clusters formed with certain "Parameters". The number of clusters according to DBSCAN, in parentheses, is the ratio of occupied clusters

Parameters (ε, $\min_{points}$)	# of total clusters	EA	randSym	randTop	RSS	GAN
$\varepsilon = 4$, $\min_{points} = 5$	12	**12 (100.0%)**	10 (83.3%)	11 (91.7%)	10 (83.3%)	**12 (100.0%)**
$\varepsilon = 3$, $\min_{points} = 5$	25	**24 (96.0%)**	22 (88.0%)	23 (92.0%)	22 (88.0%)	**24 (96.0%)**
$\varepsilon = 2$, $\min_{points} = 3$	39	32 (82.1%)	26 (66.7%)	30 (76.9%)	26 (66.7%)	**33 (84.6%)**

constraints may become more significant in determining accessible metastable structures.

3.4 Space groups

Space group selection plays a crucial role in crystal structure prediction (CSP), since certain crystal structures can only be realized within specific space groups. While structural diversity is often evaluated based on local atomic environments, it is also important to assess diversity in terms of space group distribution. To capture this aspect, we calculated the number of unique space groups of polymorphs generated by each CSP method. The results are summarized in Table 5, with a detailed list provided in the SI.

Table 5 The number of unique space groups discovered by each CSP method. Unique space groups of meta-stable polymorphs from each model were counted to measure the structural diversity of discovered polymorphs

Name	V_5O_8	V_3O_4
EA	7	24
randSym	12	27
randTop	7	20
RSS	24	**33**
GAN	6	25
VAE	4	7

For both V–O compositions, RSS produced the most diverse set of polymorphs in terms of space groups, followed by methodologically very similar randSym. To further analyze this, we plotted the distribution of space groups among the meta-stable V–O polymorphs. As shown in Fig. 4, most methods other than RSS predominantly generated low symmetry structures, such as those in the *P*1 and *Pm* space groups. Notably, when we defined high symmetry structures as those with a space group number greater than or equal to 62 (*i.e.*, ≥62),[38] over 11% of the polymorphs discovered by RSS fell into this category. A similar trend was observed in V_3O_4, as shown in Fig. S5. The higher space group diversity in RSS and randSym can be attributed to their use of symmetry constraints during initial structure selection. However, unlike RSS, which directly optimizes the initial structures and preserves their symmetry, randSym structures during relaxation are allowed to distort and lower the original symmetry.

Although the GAN model showed high structural diversity in terms of chemical space coverage, it showed relatively low

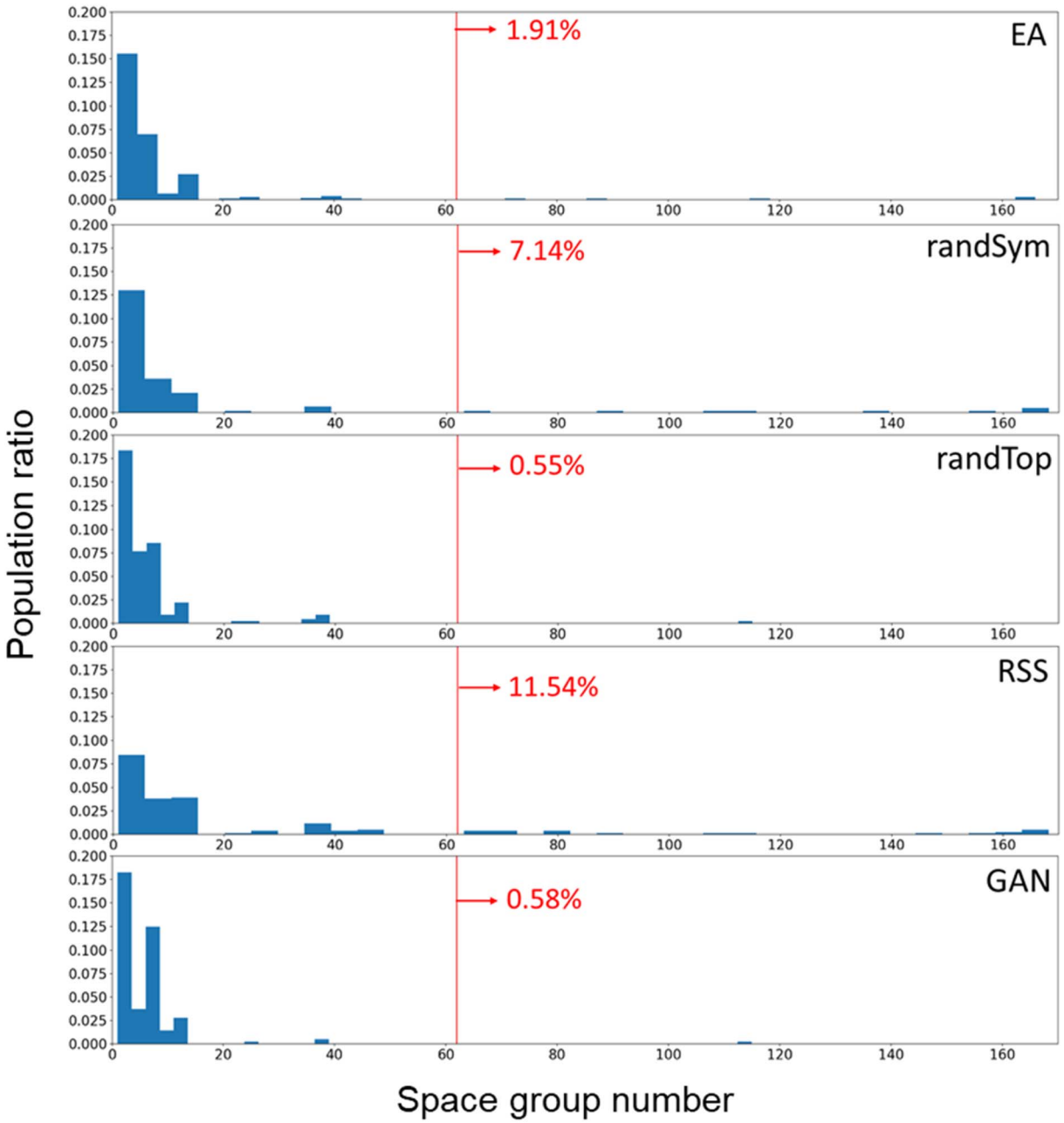

Fig. 4 Histograms for the space group of metastable V_5O_8 polymorphs. The red vertical line indicates a high symmetry space group (≥62), and the percentile in each graph means the ratio of the structures having a high symmetry space group. The *x*-axis represents the number corresponding to space groups of crystal structures, and the *y*-axis represents the ratio of frequency.

diversity in space groups (Fig. S6). The scarcity of high-symmetry structures seems to stem from the generation of structures based solely on atomic coordinates without explicit symmetry constraints. In contrast, the results of PyXtal and CSPML (Fig. S7) exhibited different trends. PyXtal produced structures with various space groups, a result of its strict adherence to the input space group during structure generation. On the other hand, CSPML showed limited space group diversity, as it generates structures based on fixed template information. To enhance space group diversity and promote the generation of high symmetry structures in deep generative models, directly incorporating symmetry information, such as the space group or Wyckoff position, into the model architecture may be a promising strategy.

4. Conclusions

In this study, we compared eight CSP methodologies, spanning traditional global optimization techniques and deep generative model-based approaches. Most methods reliably identified metastable structures (<200 meV per atom), with over half successfully predicting the ground-state structures. Notably, the VAE model identified the ground state in both test systems despite generating fewer structures, while PyXtal excelled at

producing symmetric structures but struggled with low-energy predictions. Symmetry-aware methods like RSS and randSym were effective in generating high-symmetry structures, whereas EA and GAN proved advantageous for discovering low-symmetry, structurally diverse polymorphs useful for high-throughput screening. Beyond ground-state recovery, these results show that CSP methods should also be evaluated based on their distributional sampling behavior, including metastable-structure fractions, energy distributions, chemical-space coverage, and space-group diversity.

CSPML was computationally efficient and capable of generating near-ground-state structures with minimal sampling, though its reliance on templates limited structural novelty. Deep generative models showed performances comparable to traditional methods and enabled rapid structure generation after training but required extensive data, training resources, and DFT-based post-processing. Their performance also diminished for larger systems due to increased atomic complexity.

Ultimately, the choice of CSP method should be guided by the system size, symmetry requirements, computational budget, and discovery goals. At the same time, the present benchmark should not be interpreted as a direct measure of experimental materials-discovery success, because synthesis feasibility, kinetic accessibility, processing conditions, and target functional properties also strongly affect whether a predicted structure can be realized. Traditional methods like EA, randTop, and RSS remain better suited for large or high-throughput systems due to their robustness and lower data demands. A key limitation of this study is the small system size and the standardized DFT post-processing, which may not fully capture each method's strengths—especially for large-scale applications. Future studies should explore method performance across broader system sizes and complexities and connect CSP benchmarks more explicitly with synthesis-aware and property-aware evaluation criteria to better inform CSP strategy selection.

Author contributions

Sunggi An: conceptualization, methodology, software, data curation, investigation, formal analysis, visualization, writing – original draft. Sungwon Kim: conceptualization, methodology, formal analysis, visualization, writing – original draft. Jinyoung Ko: software (DFT), investigation. Juhwan Noh: methodology, investigation. Zahed Allahyari: resources, investigation, writing-editing. Artem R. Oganov: conceptualization, methodology, supervision, writing – review and editing. Alan Aspuru-Guzik: conceptualization, methodology, supervision, writing – review and editing. Chris J. Pickard: conceptualization, methodology, supervision, writing – review and editing. Yousung Jung: conceptualization, methodology, supervision, project administration, funding acquisition, writing – review and editing.

Conflicts of interest

There are no conflicts to declare.

Data availability

All input data, DFT-relaxed crystal structures, metadata tables, grouping tables, DFT input settings, and analysis scripts used to validate and reproduce the main post-processing analyses in this study have been deposited in Zenodo at DOI: https://doi.org/10.5281/zenodo.20485770 (https://zenodo.org/records/20485770). The repository is organized into a structured project directory containing method-specific relaxed CIF structures for each composition, metadata linking each structure to its CSP method, energy, volume, and space group, and scripts for energy-above-hull analysis, SOAP descriptor generation, DBSCAN/t-SNE clustering, space-group identification, XRD generation, and figure-related post-processing. Full raw VASP output directories and some large intermediate files, such as precomputed SOAP descriptor arrays, are not included because of their large size; however, the provided DFT input settings, relaxed structures, metadata tables, and scripts allow the reported analyses to be validated and the intermediate descriptors to be regenerated if required.

The supporting figures and information of this study are provided in the supplementary information (SI). Supplementary information: supplementary figures (*e.g.*, XRD patterns, t-SNE/SOAP analyses, and DBSCAN clustering results), space-group lists for each CSP method, and DFT calculation details. See DOI: https://doi.org/10.1039/d6dd00136j.

Acknowledgements

This research was supported by the National Research Foundation of Korea (NRF) funded by the Ministry of Science and ICT (RS-2025-00514706, RS-2023-00283902 & RS-2024-00464386).

References

1 L. Pauling, *The Nature of the Chemical Bond and the Structure of Molecules and Crystals: An Introduction to Modern Structural Chemistry*, Cornell University Press, 1960.
2 A. R. Oganov, *Modern Methods of Crystal Structure Prediction*, John Wiley & Sons, 2011.
3 D. J. Wales and J. P. K. Doye, Global Optimization by Basin-Hopping and the Lowest Energy Structures of Lennard-Jones Clusters Containing up to 110 Atoms, *J. Phys. Chem. A*, 1997, **101**(28), 5111–5116, DOI: 10.1021/jp970984n.
4 J. Pannetier, J. Bassas-Alsina, J. Rodriguez-Carvajal and V. Caignaert, Prediction of Crystal Structures from Crystal Chemistry Rules by Simulated Annealing, *Nature*, 1990, **346**(6282), 343–345, DOI: 10.1038/346343a0.
5 J. C. Schön and M. Jansen, First Step Towards Planning of Syntheses in Solid-State Chemistry: Determination of Promising Structure Candidates by Global Optimization, *Angew Chem. Int. Ed. Engl.*, 1996, **35**(12), 1286–1304, DOI: 10.1002/anie.199612861.
6 T. S. Bush, C. R. A. Catlow and P. D. Battle, Evolutionary Programming Techniques for Predicting Inorganic Crystal Structures, *J. Mater. Chem.*, 1995, **5**(8), 1269–1272, DOI: 10.1039/JM9950501269.

7 A. R. Oganov, A. O. Lyakhov and M. Valle, How Evolutionary Crystal Structure Prediction Works—and Why, *Acc. Chem. Res.*, 2011, **44**(3), 227–237, DOI: 10.1021/ar1001318.

8 C. W. Glass, A. R. Oganov and N. Hansen, USPEX—Evolutionary Crystal Structure Prediction, *Comput. Phys. Commun.*, 2006, **175**(11), 713–720, DOI: 10.1016/j.cpc.2006.07.020.

9 A. R. Oganov, Y. Ma, A. O. Lyakhov, M. Valle and C. Gatti, Evolutionary Crystal Structure Prediction as a Method for the Discovery of Minerals and Materials, *Rev. Mineral. Geochem.*, 2010, **71**(1), 271–298, DOI: 10.2138/rmg.2010.71.13.

10 A. O. Lyakhov and A. R. Oganov, Evolutionary Search for Superhard Materials: Methodology and Applications to Forms of Carbon and TiO$\{\}_\{2\}$, *Phys. Rev. B:Condens. Matter Mater. Phys.*, 2011, **84**(9), 092103, DOI: 10.1103/PhysRevB.84.092103.

11 C.-H. Hu, A. R. Oganov, Q. Zhu, G.-R. Qian, G. Frapper, A. O. Lyakhov and H.-Y. Zhou, Pressure-Induced Stabilization and Insulator-Superconductor Transition of BH, *Phys. Rev. Lett.*, 2013, **110**(16), 165504, DOI: 10.1103/PhysRevLett.110.165504.

12 K. Dolui, L. J. Conway, C. Heil, T. A. Strobel, R. P. Prasankumar and C. J. Pickard, Feasible Route to High-Temperature Ambient-Pressure Hydride Superconductivity, *Phys. Rev. Lett.*, 2024, **132**(16), 166001, DOI: 10.1103/PhysRevLett.132.166001.

13 C. Hong, J. M. Choi, W. Jeong, S. Kang, S. Ju, K. Lee, J. Jung, Y. Youn and S. Han, Training Machine-Learning Potentials for Crystal Structure Prediction Using Disordered Structures, *Phys. Rev. B*, 2020, **102**(22), 224104, DOI: 10.1103/PhysRevB.102.224104.

14 T. Long, N. M. Fortunato, I. Opahle, Y. Zhang, I. Samathrakis, C. Shen, O. Gutfleisch and H. Zhang, Constrained Crystals Deep Convolutional Generative Adversarial Network for the Inverse Design of Crystal Structures, *npj Comput. Mater.*, 2021, **7**(1), 1–7, DOI: 10.1038/s41524-021-00526-4.

15 I.-H. Lee and K. J. Chang, Crystal Structure Prediction in a Continuous Representative Space, *Comput. Mater. Sci.*, 2021, **194**, 110436, DOI: 10.1016/j.commatsci.2021.110436.

16 C. J. Court, B. Yildirim, A. Jain and J. M. Cole, 3-D Inorganic Crystal Structure Generation and Property Prediction via Representation Learning, *J. Chem. Inf. Model.*, 2020, **60**(10), 4518–4535, DOI: 10.1021/acs.jcim.0c00464.

17 S. Kim, J. Noh, G. H. Gu, A. Aspuru-Guzik and Y. Jung, Generative Adversarial Networks for Crystal Structure Prediction, *ACS Cent. Sci.*, 2020, **6**(8), 1412–1420, DOI: 10.1021/acscentsci.0c00426.

18 J. Noh, J. Kim, H. S. Stein, B. Sanchez-Lengeling, J. M. Gregoire, A. Aspuru-Guzik and Y. Jung, Inverse Design of Solid-State Materials via a Continuous Representation, *Matter*, 2019, **1**(5), 1370–1384, DOI: 10.1016/j.matt.2019.08.017.

19 S. Fredericks, K. Parrish, D. Sayre and Q. Zhu, PyXtal: A Python Library for Crystal Structure Generation and Symmetry Analysis, *Comput. Phys. Commun.*, 2021, **261**, 107810, DOI: 10.1016/j.cpc.2020.107810.

20 M. Kusaba, C. Liu and R. Yoshida, Crystal Structure Prediction with Machine Learning-Based Element Substitution, *Comput. Mater. Sci.*, 2022, **211**, 111496, DOI: 10.1016/j.commatsci.2022.111496.

21 X. Luo, Z. Wang, P. Gao, J. Lv, Y. Wang, C. Chen and Y. Ma, Deep Learning Generative Model for Crystal Structure Prediction, *npj Comput. Mater.*, 2024, **10**(1), 1–10, DOI: 10.1038/s41524-024-01443-y.

22 J. Pickard and C. Beyond, Theory-Driven Discovery: Introducing Hot Random Search and Datum-Derived Structures, *Faraday Discuss.*, 2025, **256**, 61–84, DOI: 10.1039/D4FD00134F.

23 A. O. Lyakhov, A. R. Oganov, H. T. Stokes and Q. Zhu, New Developments in Evolutionary Structure Prediction Algorithm USPEX, *Comput. Phys. Commun.*, 2013, **184**(4), 1172–1182, DOI: 10.1016/j.cpc.2012.12.009.

24 P. V. Bushlanov, V. A. Blatov and A. R. Oganov, Topology-Based Crystal Structure Generator, *Comput. Phys. Commun.*, 2019, **236**, 1–7, DOI: 10.1016/j.cpc.2018.09.016.

25 C. J. Pickard and R. J. Needs, High-Pressure Phases of Silane, *Phys. Rev. Lett.*, 2006, **97**(4), 045504, DOI: 10.1103/PhysRevLett.97.045504.

26 C. J. Pickard and R. J. Needs, Ab Initio Random Structure Searching, *J. Phys.:Condens. Matter*, 2011, **23**(5), 053201, DOI: 10.1088/0953-8984/23/5/053201.

27 S. P. Ong, W. D. Richards, A. Jain, G. Hautier, M. Kocher, S. Cholia, D. Gunter, V. L. Chevrier, K. A. Persson and G. Ceder, Python Materials Genomics (Pymatgen): A Robust, Open-Source Python Library for Materials Analysis, *Comput. Mater. Sci.*, 2013, **68**, 314–319, DOI: 10.1016/j.commatsci.2012.10.028.

28 A. Merchant, S. Batzner, S. S. Schoenholz, M. Aykol, G. Cheon and E. D. Cubuk, Scaling Deep Learning for Materials Discovery, *Nature*, 2023, **624**(7990), 80–85, DOI: 10.1038/s41586-023-06735-9.

29 I. Gulrajani, F. Ahmed, M. Arjovsky, V. Dumoulin and A. C. Courville, Improved Training of Wasserstein GANs, in *Advances in Neural Information Processing Systems*, Curran Associates, Inc., 2017, vol. 30.

30 D. P. Kingma and M. Welling, Auto-Encoding Variational Bayes, *International Conference on Learning Representations (ICLR)*, 2014, DOI: 10.48550/arXiv.1312.6114.

31 R. Zhu, W. Nong, S. Yamazaki and K. Hippalgaonkar, Wyckoff Inorganic Crystal Generator Framework, *Matter*, 2024, **7**(10), 3431–3445, DOI: 10.1016/j.matt.2024.05.042.

32 Z. Ren, S. I. P. Tian, J. Noh, F. Oviedo, G. Xing, J. Li, Q. Liang, R. Zhu, A. G. Aberle, S. Sun, X. Wang, Y. Liu, Q. Li, S. Jayavelu, K. Hippalgaonkar, Y. Jung and T. Buonassisi, An Invertible Crystallographic Representation for General Inverse Design of Inorganic Crystals with Targeted Properties, *Matter*, 2022, **5**(1), 314–335, DOI: 10.1016/j.matt.2021.11.032.

33 W. Sun, S. T. Dacek, S. P. Ong, G. Hautier, A. Jain, W. D. Richards, A. C. Gamst, K. A. Persson and G. Ceder, The Thermodynamic Scale of Inorganic Crystalline

Metastability, *Sci. Adv.*, 2016, **2**(11), e1600225, DOI: 10.1126/sciadv.1600225.
34 A. Reinhardt, C. J. Pickard and B. Cheng, Predicting the Phase Diagram of Titanium Dioxide with Random Search and Pattern Recognition, *Phys. Chem. Chem. Phys.*, 2020, **22**(22), 12697–12705, DOI: 10.1039/D0CP02513E.
35 A. P. Bartók, R. Kondor and G. Csányi, On Representing Chemical Environments, *Phys. Rev. B:Condens. Matter Mater. Phys.*, 2013, **87**(18), 184115, DOI: 10.1103/PhysRevB.87.184115.
36 G. C. Linderman and S. Steinerberger, Clustering with T-SNE, Provably, *SIAM Journal on Mathematics of Data Science*, 2019, **1**(2), 313–332, DOI: 10.1137/18M1216134.
37 M. Ester, H.-P. Kriegel and X. Xu, *A Density-Based Algorithm for Discovering Clusters in Large Spatial Databases with Noise*.
38 Y. Zhao, E. M. D. Siriwardane, Z. Wu, N. Fu, M. Al-Fahdi, M. Hu and J. Hu, Physics Guided Deep Learning for Generative Design of Crystal Materials with Symmetry Constraints, *npj Comput. Mater.*, 2023, **9**(1), 1–12, DOI: 10.1038/s41524-023-00987-9.
39 P. Hu, P. Hu, T. Duc Vu, M. Li, S. Wang, Y. Ke, X. Zeng, L. Mai and Y. Long, Vanadium oxide: phase diagrams, structures, synthesis, and applications, *Chem. Rev.*, 2023, **123**(8), 4353–4415.